KE GAO[1*], QIWEN LI[1], LIANZENG SHI[1],
AOBO YANG[1], ZHIPENG QI[1]

STUDY OF THE FLOW FIELD AND PERMEABILITY CHARACTERISTICS IN THE GOAF USING THE OPENPNM PACKAGE

The roof-caving step scale goaf behind the working face is sensitive to the region's spontaneous combustion and gas concentration distribution, including many rock block cracks and holes. A severe deviation from the dynamics of fluids in porous media by representative element volume (REV), leading to the results of Computational Fluid Dynamics (CFD) simulation, has a significant error. A heterogeneous two-dimensional pore network model was established to simulate the goaf flow accurately. The network was first created using the simple cubic lattice in the OpenPNM package, and the spatial distribution of the "O-ring" bulking factor was mapped to the network. The bulking factor and Weibull distribution were combined to produce the size distribution of the pore and throat in the network. The constructed pore network model was performed with single-phase flow simulations. The study determined the pore structure parameters of the pore network through the goaf's risked falling characteristics and described the flow field's distribution characteristics in the goaf. The permeability coefficient increases as pore diameter, throat diameter, pore volume and throat volume increase and increases as throat length decreases. The correlation between throat volume and permeability coefficient is the highest, which indicates that the whole throat is the main control factor governing the air transport capacity in the goaf. These results may provide some guidelines for controlling thermodynamic disasters in the goaf.

Keywords: goaf of longwall face; pore network model; OpenPNM open-source package; "O-ring" shape of goaf permeability; Weibull distribution; permeability characteristics

Nomenclature

K_P — bulking factor distribution function,
$K_{P,\max}$ — initial bulking factor,

---

[1] LIAONING TECHNICAL UNIVERSITY, COLLEGE OF SAFETY SCIENCE AND ENGINEERING, KEY LABORATORY OF MINE THERMODYNAMIC DISASTERS AND CONTROL OF MINISTRY OF EDUCATION, CHINA

* Corresponding author: gaoke@lntu.edu.cn

$K_{P,\min}$ –   compaction bulking factor,

a_0, a_1 –   bulking factor attenuation ratios (m^{-1}),

d_0, d_1 –   specific spatial distances (m),

ξ_1 –   adjustment factor of distribution,

μ –   air dynamic viscosity (Pa·s),

v –   air velocity (m/s),

p –   air pressure (Pa),

q –   flow rate through a pore conduit (m^3/s),

g –   permeability coefficient (m^3/(Pa·s)),

L –   length of the conduit (m),

κ –   shape parameter,

λ –   scale parameter,

V –   volume (m^3),

X –   lattice size in x-direction no. of pores,

Y –   lattice size in y-direction no. of pores,

Z –   lattice size in z-direction no. of pores,

L_C –   lattice constant (m),

L' –   length of the working face (m),

r –   roadway ventilation resistance at per unit length (N·s^2/m^9),

Q –   airflow rate along working face (m^3/min).

1. Introduction

After mining out the coal seam, the immediate roof, the basic roof and the main roof collapsed under mine pressure, forming the extremely complex, irregular and variable goaf composed of the residual coal and broken rock in the mining process of working face. A large amount of residual coal is scattered in the goaf, which can easily produce thermodynamic disasters, such as residual coal oxidation and spontaneous combustion, gas combustion explosions and coal dust explosions. An accurate grasp of the fluid flow and energy mass transfer law in the goaf is a prerequisite for the pre-control of thermodynamic disasters [1].

Scholars have conducted many preliminary studies on the flow field in the goaf based on the fluid dynamics of porous media. The inaccessibility of the goaf for personnel is due to its complex and specific nature. Most of the current research on the flow field and gas transport law in the goaf focuses on theoretical models and numerical simulation studies, although field measurements of the permeability of goafs are known [2]. However, much more research is conducted using numerical methods. Academician Qian [3] proposed the "O-ring" risked falling compaction character, which laid the foundation for the subsequent research of permeability characteristics. Li et al. [4] proposed a step model for the bulking factor in the goaf by using the theory of "horizontal three zones" of rock formation moving and breaking. They also provided a theoretical solution for the void permeability in different fracture development zones and considered the porosity and permeability to be constants in each subzone. Liang et al. [5] constructed a two-dimensional heterogeneous continuous distribution model of porosity and permeability in the collapse zone using roof strata collapse theory. Based on this model, they simulated the distribution law of the air leakage flow field. Some scholars have constructed

a three-dimensional mathematical model of the heterogeneous porous media for the goaf caving based on the "O-ring" theory and have used the Kozeny-Carman equation or its modified forms to calculate the permeability of the goaf [6-8].

The mainstream method used by the scholars mentioned above to carry out seepage simulation is still to use CFD software or to estimate the permeability of the goaf based on the Kozeny-Carman (KC) equation. Traditional CFD methods (e.g., FLUENT, COMSOL, etc.) use a continuous medium model to solve mass, momentum, and species balances through constitutive equations, such as a simple extension to Darcy's law for multiphase flows [9,10]. However, this approach faces difficulties considering complex porous media morphologies with different heterogeneity. Each modelled phenomenon requires experimental measurements to describe the constitutive relationships of the macroscopic transport properties of the medium, such as permeability, wetting or effective diffusion coefficient [11,12]. The permeability of the goaf is challenging to measure in the laboratory due to its complex and irregular pore structure. Therefore, CFD scholars often use the KC equation to estimate the permeability of the goaf, which is then used as a UDF (User-Defined Function) input when constructing the porous media model. The limitations of KC as a semi-empirical equation have been widely demonstrated [13,14]. In addition to the abovementioned problems, conventional CFD methods treat porous media as volume-averaged continua without decomposing microscale features, making it difficult to achieve results associated with microscale structures [15,16]. The goaf is a three-dimensional, multi-connected, complex internal flow field bounded by various structures. Scholars in China and abroad are using porous medium continuous medium fluid dynamics theory and simulation technology to study the gas flow state in the goaf. That is, a hypothetical continuous medium is used instead of a porous medium full of voids, and the average value of state variables, such as physical parameters of the porous medium over a certain volume (REV), is used as the value of the parameters of the hypothetical continuous body. However, the fluid space in the goaf consists of residual coal microporosity, inter-rock crevices and pores, and the fluid flow does not necessarily occur through the caved rock in the goaf. The rock fractures and pores are the leading cause of fluid flow in the goaf, significantly affecting it. Their size range varies widely, and the pores can even reach several meters, far beyond the pores' scale in porous media. And they cannot be expressed in REV or abstractly averaged. Therefore, using porous media fluid dynamics theory, the goaf flow field calculation in a fully mechanized caving coal mine may differ significantly from the actual flow field.

With the development of computer hardware and various numerical simulation methods, pore network modelling (PNM) has become a critical method for studying the seepage process of coal rocks because it can connect microscopic pore structures and macroscopic seepage characteristics [17]. Since Fatt [18] pioneered PNM, its effectiveness and low cost have made it a well-established and long-standing method for simulating transport in porous materials [19,20]. To better characterize the pores, the researchers discretize the pore space into interconnected pores and throats, where spheres represent the pores, and tetrahedra, rectangles or cylinders represent the throats. PNMs represent an alternative approach to the more widely used continuum model. Their main difference lies in handling the transport properties between two physical locations in the domain. In the continuous medium model, the flow rate or pressure drop between two adjacent locations is determined by the permeability of the medium [12]. From the limitations of permeability described above, it is clear that the pressure and gas velocity calculated by CFD for the goaf may differ from the actual results. In PNM, the two

adjacent positions of the throat connection are considered the actual pores. PNM transforms the flow problem into a pipe network or resistor network problem by assigning a permeability coefficient (also called hydraulic conductivity [21]) to pores and throats [22]. The flow between these two pores is considered to flow through the pipe and can be described by various analytical solutions. The PNM approach can directly incorporate the structure and topology of porous media into the model, establishing a direct link to the gas transport process instead of relying on constitutive relationships [23].

Based on the above discussion, PNM can describe the pore structure of porous media more accurately and efficiently. Pore structure refers to the composition of the pores of porous media, including characteristics such as the size, shape, and connectivity of pores and throats [24]. The transport properties, such as the porosity and permeability coefficient of the goaf, determine the seepage characteristics of the gas in the goaf, and these transport properties depend on the geometric properties and topology of the pore space in the goaf [25]. Therefore, to predict the seepage characteristics of a goaf, it is essential to analyze the pore space of the goaf quantitatively, select the appropriate information regarding the pore structure to establish relevant models and conduct the studies on the seepage at the pore scale. This has important theoretical and practical significance for solving engineering problems such as mine construction and thermodynamic disaster prevention and control.

This paper presents the PNM method using open source OpenPNM package [12] to perform pore network simulation based on the "O-ring" theory in the goaf. The Hagen-Poiseuille law describes the single-phase flow in the pore space of the goaf. Combined with the Stokes flow algorithm [12,20], this study investigates the flow field distribution and permeability characteristics of the goaf at the pore scale. It quantitatively examines the relationship between transport properties and pore structure in the goaf.

2. Background

2.1. Mathematical model of the bulking factor of the goaf

Considering the mining conditions of the 2220 working face [26,27] in the Linnancang mine, the mine is a low-gas mine. The fully mechanized top coal caving technology is applied to the 2220 working face, and the roof of the goaf is treated by caving method. The length of the working face is 80 m, the thickness of the coal seam is 4.6 m, the mining height is 2.2 m, and the length of the goaf is 200 m, as shown in Fig. 1. The figure shows that q_L and q_L' are the leakage amount of inflow and outflow, respectively, m^3/s.

The overlying strata of the goaf collapse with the advancement of the working face, and the cave goes from stable to unstable and then to stable process. Due to the support of the coal wall around the goaf, the risked falling area forms the main roof and the overlying key strata, which have "O-X" shaped rupture. With the advancement of the working face and pressure cycle, the central mining fractures and the free-caved rocks are compacted. While on the side of the surrounding coal column, bed separation fractures and caving-prone fractures will be maintained, thus forming a continuous fracture development zone around the goaf, called the mining fracture "O-ring", which is the main channel of air leakage and seepage in the goaf [2]. According to the law of mine pressure observation, the characteristic equation of the distribution of the two-
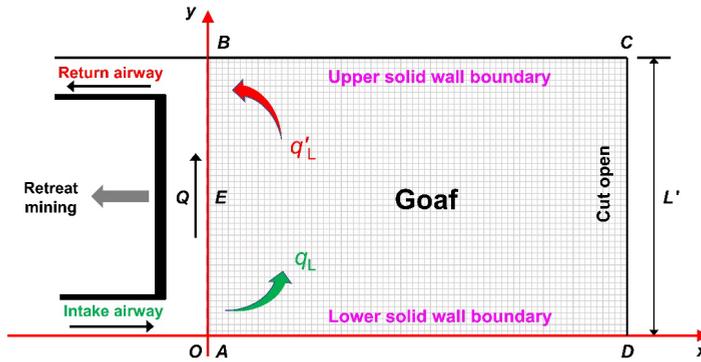
Fig. 1. Geometric model of the goaf flow field

dimensional "O-ring" bulking factor between the caving zone and compaction zone in the goaf can be expressed as [26], with the dynamic change of the working face advancement:

$$K_p(x,y) = K_{p,\min} + \left(K_{p,\max} - K_{p,\min}\right) \times \exp\left(-a_1 d_1 \left(1 - e^{-\xi_1 a_0 d_0}\right)\right) \tag{1}$$

where K_P is the bulking factor of caved rock in the goaf (distribution function), dimensionless, $K_{P,\max}$ is the initial bulking factor, dimensionless, $K_{P,\min}$ is the compaction bulking factor, dimensionless, a_0 and a_1, respectively, are the attenuation rates from the wall of the solid rock and the working surface, m^{-1}, d_0 and d_1, respectively, are the distances from point (x,y) to the supporting coal pillar and the longwall face, m, ξ_1 is the adjustment number to control the distribution pattern of the "O-ring" model, dimensionless, which can be determined by trial calculation until it meets the actual situation (the larger ξ_1 is, the more square-angled "O-ring" is). For the 2220 working face, $a_1 = 0.0368$ m^{-1}, $a_0 = 0.268$ m^{-1} and $\xi_1 = 0.233$, and $K_P(x,y)$ distribution is shown in Fig. 2.
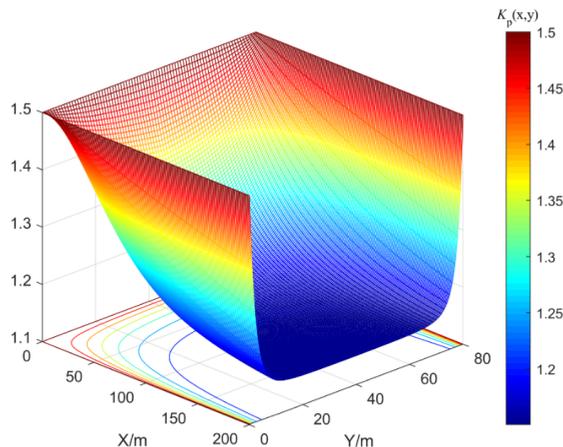
Fig. 2. Bulking factor K_P distribution of "O-ring"

2.2. Local scale

This paper investigates the single-phase, isothermal, incompressible airflow in the goaf, which is an undeformable porous medium, where the local equation governs mass conservation.

$$\nabla \cdot v = 0 \tag{2}$$

where v is the local velocity of the airflow, m/s.

The conservation of momentum equation governs the airflow motion in the goaf.

$$\mu \nabla^2 v = \nabla p \tag{3}$$

where μ is the dynamic viscosity of the air, Pa·s and p is its local pressure, Pa.

2.3. Pore scale

Given the steady-state Stokes flow of a Newtonian fluid (Eqs. (2) and (3)), the following mass conservation equation is applied to each pore in the pore network. Solving this linear system of equations enables the determination of the flow rate and pressure drop:

$$q_i = \sum_{j=1}^{n_i} g_{ij} \left(p_j - p_i \right) = 0 \tag{4}$$

where i and j denote the pores and neighboring ones to be considered, n_i is the number of pores neighboring to pore i, q_i is the net flow rate through pore i, m³/s, g_{ij} is the permeability coefficient for flow between pore i and neighboring pore j, m³/(Pa·s), p_i and p_j are the pressures in each pore, Pa. Fig. 3 shows schematic diagram of two neighboring pore bodies and connecting throat. The assembly is made of throat ij and halves of the neighbor pores i and j of diameters d_{ij}, d_i, and d_j and lengths L_{ij}, L_i, and L_j.
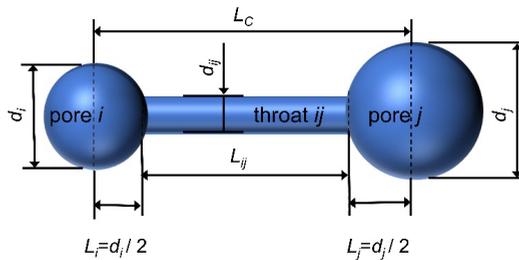

Fig. 3. Dimensional schematic diagram of the pore-throat-pore assembly

The permeability coefficient, g, of the pores and throats can be calculated using the Hagen-Poiseuille model [28] as follows:

$$g = \frac{\pi d^4}{128 \mu L} \tag{5}$$

where μ is the dynamic viscosity, Pa·s, g is the permeability coefficient of the conduit, m³/(Pa·s), d and L, respectively, are the diameter and the length of the conduit, m. The total permeability coefficient for flow between two adjacent objects is utilized as the net permeability coefficient for flow through half of pore i, the connecting throat, and half of pore j. The permeability coefficient for each section, is calculated using Eq. (5), and the pore-throat-pore assembly's net permeability coefficient is derived from the linear resistance theory of series resistance [29] as follows:

$$g_{ij} = \left(\frac{1}{g_i} + \frac{1}{g_{t,ij}} + \frac{1}{g_j} \right)^{-1} \tag{6}$$

3. Pore network model based on Weibull distribution

Based on bulking factor K_P distribution of the caved rocks in the goaf, Weibull distribution was adopted to simulate the spatial heterogeneity of the bulking factor, combined with the PNM method, then the spatial distribution law of the pore structure in the heterogeneous goaf was simulated, and the pore network model in the goaf was established.

3.1. Network creation

In this study, OpenPNM package was used to perform pore network simulations in the goaf of the 2220 working face in the Linnancang mine to study the flow field and permeability characteristics. To obtain a more suitable porosity for the "O-ring" goaf and to easily calculate transport equations, spheres and cylinders were chosen for the pore and throat, respectively. For the network a domain size of $200 \times 80 \times 1$ m filled with 16,000 pores and 31,720 throats was created using OpenPNM's Cubic, and the network spacing was set to 1 m.

3.2. Weibull distribution

The Weibull cumulative distribution function is widely used in pore network modeling due to its mathematical simplicity, flexibility and reliability [30]. The two-parameter Weibull distribution is utilized to construct pore network model by assigning pore and throat dimensions [29]:

$$b_{p,i} = \lambda \left[-\ln\left(1 - \chi\right) \right]^{-1/\kappa} + b_{\min} \tag{7}$$

where $b_{p,i}$ is the radius of the ith pore, m, χ is considered as the "pore seed" value in OpenPNM, which means to generate pore seeds that are spatially correlated with their neighbors, $b_{\min}$ is the minimum pore radius, m, κ is the Weibull modulus that controls the shape of the distribution and indicates the degree of dispersion of the pore diameter distribution. The smaller κ, the higher the dispersion of the pore diameter distribution. And λ is the scale parameter of the average value of the bulking factor which is used to describe the caving degree of the caved rock in the goaf.

To construct a pore network model of the "O-ring" goaf, the value of Eq. (1) should be assigned to χ, like pn['pore.seed']* = np.flatten($K_P(x,y)$). This requires that Fig. 2 should also be generated from a grid of $200 \times 80 \times 1$ size with a total of 16,000 grid positions in order to achieve a one-to-one correspondence between the values of the bulking factor K_P and the "pore seed".

58

3.3. Porosity

The porosity not only affects the regular mining of coal seams but also influences the permeability characteristics of the goaf after mining, and can reflect the heterogeneity of the goaf [8,31]. The following equation is used to calculate the porosity (ε) of the network for the void volume:

$$\varepsilon = \frac{V_p + V_t}{L_C^3 XYZ} \tag{8}$$

where V_p is the network's pore volume, m³, V_t is the throat volume, m³, X, Y and Z are the network dimensions expressed in the number of pores, dimensionless, and L_C is the lattice constant, m. In this study, the lattice constant is kept consistent with the set grid spacing of the goaf with a value of 1 m. Since the model is a two-dimensional pore network model, Z is 1. The number and location of control pores and throats can be modified by setting the "label" in OpenPNM package and then combining it with Eq. (7) to calculate the porosity at any location in the pore network.

3.4. Pore and throat size distributions

Firstly, np.flatten($K_P(x,y)$) was summed and averaged, which determined the scale parameter, $\lambda = 1.244$. The shape parameter $\kappa = 1.41$ was obtained by solving Eqs. (1), (7) and (8). In the next step, the L_C was verified to be greater than the largest pore size in the network to prevent the overlap. Once the pore size was determined, the throat size was calculated using a function based on the smaller value of the neighboring pores, $d_{ij} = \min\{b_{p,i}, b_{p,j}\}$, where d_{ij} is the diameter of the throat. The two-dimensional pore network model with pore diameters and throat diameters in the range of 0.025-0.049 m is shown in Fig. 4. Fig. 5 presents the histograms of pore diameter, coordination numbers, throat diameter and length for the corresponding model. Figs. 4-5 demonstrate that the highest percentage of small-sized pores or throats is located in the recompacted zone in the goaf, while the fracture development zone is characterized by the distribution of large-sized pores or throats. This is due to the mining process resulting in varying
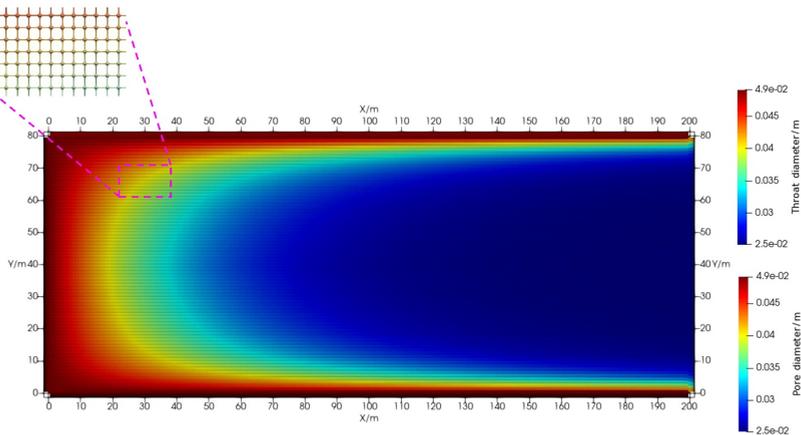

Fig. 4. Two-dimensional pore network model in the goaf

degrees of pore structure development within different zones of the goaf. The size distribution of the pore structure validates the risked falling characteristics and heterogeneity of the goaf.
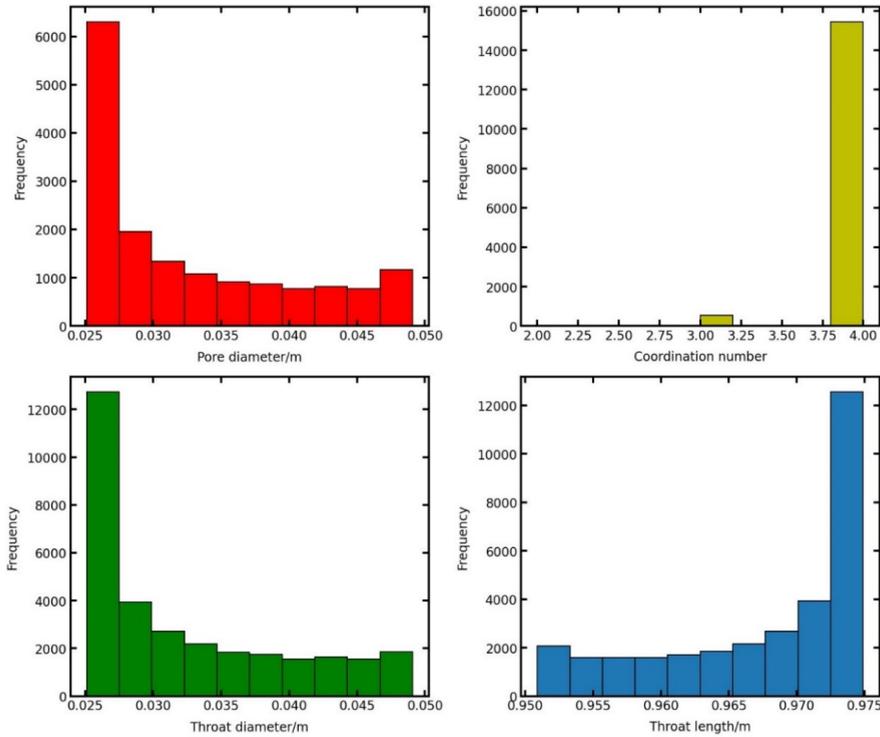

Fig. 5. Histogram of pore diameter, coordination number, throat diameter and throat length

3.5. Boundary value problem

The schematic diagram of the flow field in the two-dimensional heterogeneous goaf is shown in Fig. 1. The air leakage is an incompressible gas seepage movement, with no horizontal leakage [32].

On the air leakage boundary AB:

$$p = (L' - y) \cdot r \cdot Q^2 \tag{9}$$

On the other boundary BCDA:

$$\frac{\partial p}{\partial n} = 0 \tag{10}$$

where p is the air pressure, Pa, L' is the length of the working face, m, r is the roadway ventilation resistance at per unit length, $\mathrm{N \cdot s^2/m^9}$, Q is the airflow rate along working face, $\mathrm{m^3/min}$, and n represents the direction normal to the boundary. Q and r, respectively, are 426.8 $\mathrm{m^3/min}$ and 0.0094 $\mathrm{N \cdot s^2/m^9}$, as obtained from field observations.

Set the inlet boundary condition of the pore network model of the goaf as the pressure inlet and the outlet boundary condition as the pressure outlet. The boundary condition parameters of the pore network model are determined using Eqs. (9) and (10). The pressure gradient in the AE section was used as the inlet boundary value, while the pressure gradient in the EB section was used as the outlet boundary value. The air temperature was 290 K, and the air viscosity was $1.834×10^{-5}$ Pa·s. The Stokes flow algorithm in OpenPNM package was used to simulate single-phase flow simulations in the goaf.

4. Results and discussion

4.1. Pressure distribution of the leakage flow field

The mass conservation equation over each pore (Eq. (4)) was solved for the given pressure boundary conditions. Then the pressure distribution in the pore network model is obtained and visualized, as shown in Fig. 6. The plotted air pressure contours are shown in Fig. 7. To study the relationship between the air pressure in the goaf and the working face advance distance, pores at $Y = 0$ m and $Y = 80$ m were selected to study the air pressure variation at both ends of the goaf. In contrast, pores at $Y = 40$ m and $Y = 41$ m were used to reflect the pressure variation in the middle of the goaf. The resulting curves are shown in Fig. 8.
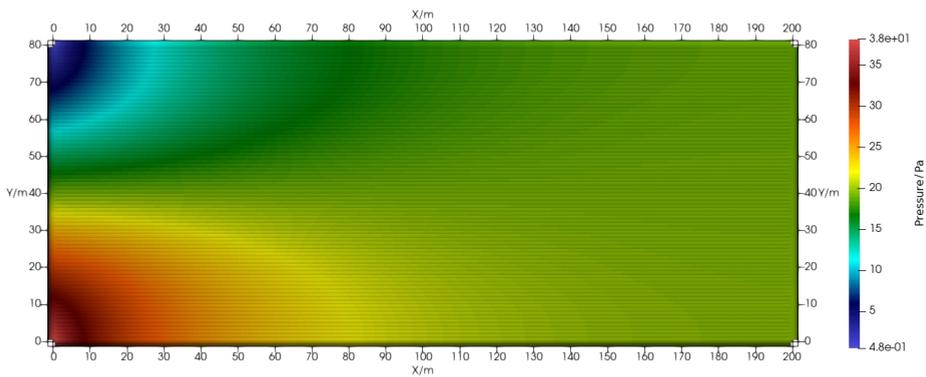

Fig. 6. Pressure distribution in the pore network model of the goaf
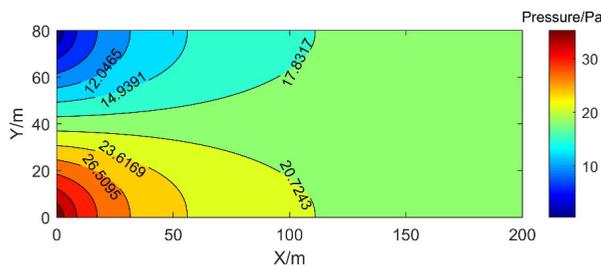

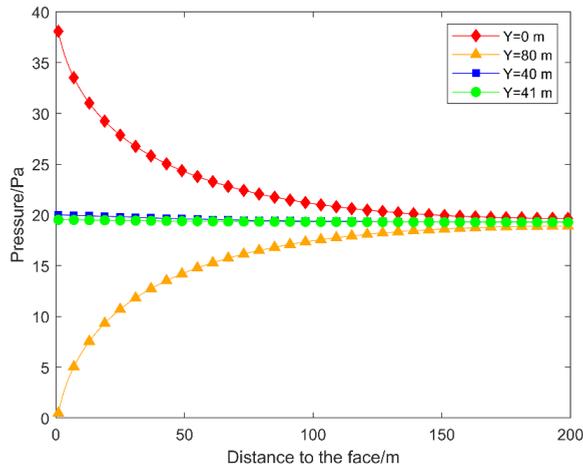Fig. 7. Contour map of air pressure distribution in the goaf

Fig. 8. Relationship between air pressure and distance to face

Figs. 6 and 7 show that the pressure at the lower corner of the inlet side of the working face is higher, and the pressure at the upper corner is lower. The two pressure curves, $Y = 0$ m and $Y = 80$ m , in Fig. 8 clearly illustrate that the air pressure gradient is the largest near the inlet side and outlet side of the working face, where the pressure drops significantly within a short distance. The air pressure gradually tends to level off after 120 m along the direction of the goaf, and there is almost no change in pressure at the deeper part of the goaf. The pressure curves at $Y = 40$ m and $Y = 41$ m show that the air pressure difference near the centerline of the working face is slight and almost unchanged.

4.2. Velocity distribution of the leakage flow field

The pore's net flow rate is zero because each pore's flow rate follows the law of mass conservation in the pore network model. Using an algorithm, the flow rate of each throat in the network can be determined. The resulting velocity distribution of the flow field in the goaf is shown in Fig. 9. The air pressure and velocity distribution are solved using the Stokes flow algorithm. These two distributions are then superimposed to obtain the flow network, as illustrated in Fig. 10.
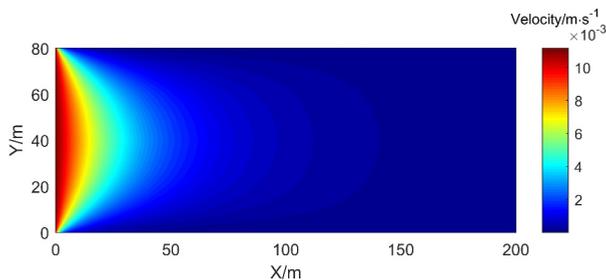

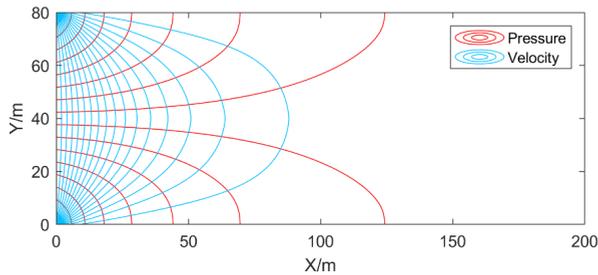Fig. 9. Air velocity distribution in the goaf

Fig. 10. Pressure and velocity profiles in the goaf

The maximum air velocity is 0.011147 m/s in Fig. 9, which coincides with the result ($v_{max} = 0.0111311$ m/s) obtained by Li et al. [26] in their simulation of the 2220 working face using a self-programmed G3 program. Moreover, similar values in the 0.01-0.03 m/s of maximum velocities for the analyzed goafs with U-type ventilation systems are presented by Szlazak et al. [33]. Fig. 11 reveals the flow state of the flow field under a heterogeneous flow field. Compared with the homogeneous flow field, the airflow movement pattern of the goaf in Fig. 10 is consistent with the changes in non-compactness. The airflow lines near the working face are significantly denser than those in the internal area, particularly at the upper and lower corners of the goaf. Some leaking airflows flow back into the working face along the boundary of the working face, and the airflow is turbulent and distributed in a circular arc. The airflow leakage seeps into the deep part of the goaf, which increases the risk of collapse. The airflow in this region is mainly in a laminar flow state with sparse flow lines.

4.3. Effect of the pore structure of the goaf on permeability characteristics

The permeability coefficient serves as a comprehensive indicator of the permeability capacity. The study utilised the Hagen-Poiseuille law to estimate the transport property. The result of solving Eqs. (5) and (6) is shown in Fig. 11. To investigate the relationship between the permeability characteristics and pore structure in the pore network model, the pores and throats at $Y = 40$ m were selected, and the fitted curves are illustrated in Fig. 12.
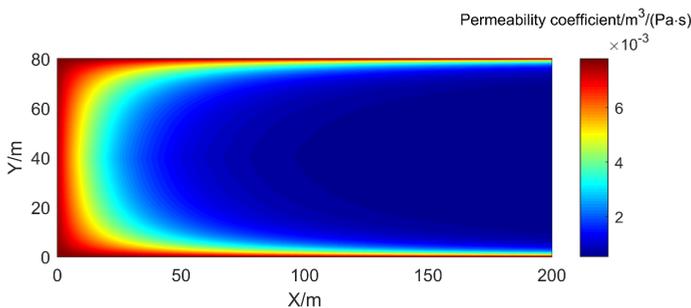

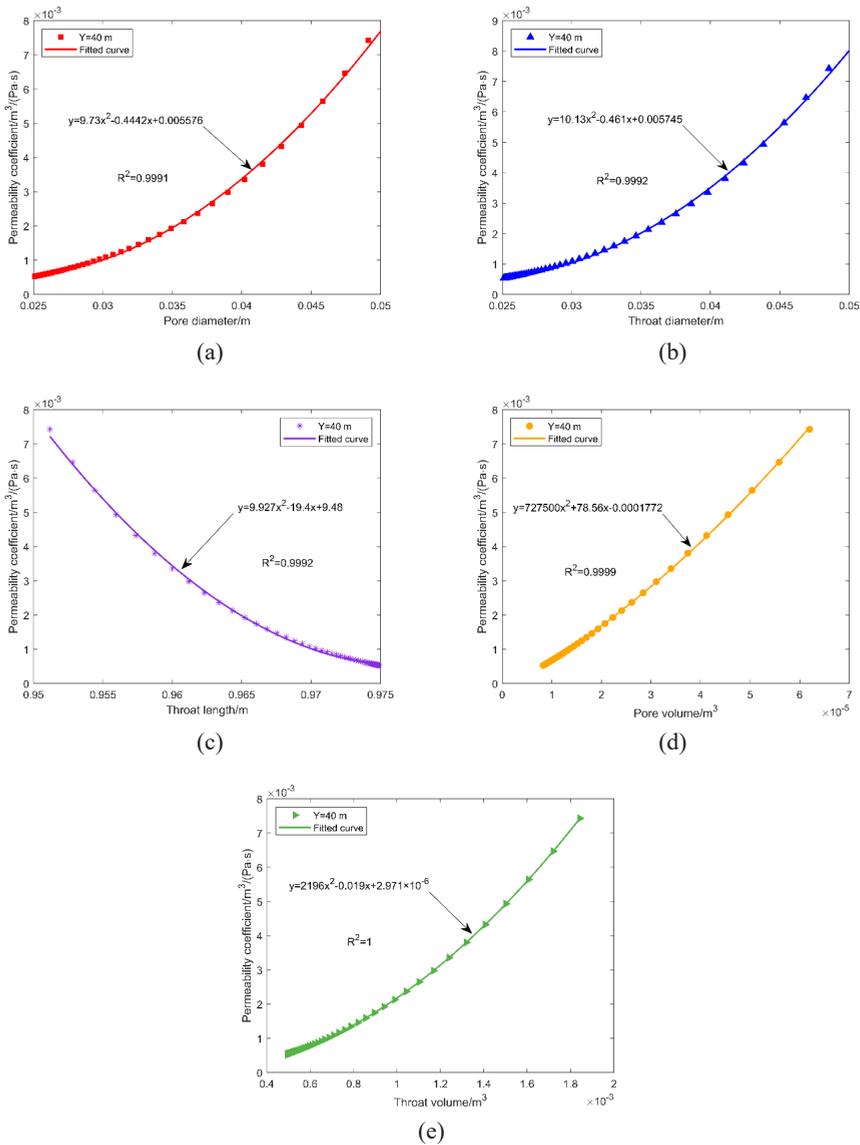Fig. 11. Permeability coefficient distribution in the goaf

Fig. 12. Relationship between permeability coefficient and the (a) pore diameter, (b) throat diameter,
(c) throat length, (d) pore volume, and (e) throat volume in the goaf

Fig. 11 shows that the permeability coefficient of the goaf ranges from 5.32×10^{-4} to 7.78×10^{-3} m³/(Pa·s). The permeability characteristics of the deep part of the goaf are very different from those near the working face. The maximum value of the permeability coefficient is located in the fracture development zone, while the minimum value is located in the recompacted zone. With the increase in the vertical distance from the mined coal seam, the permeability coefficient of the recompacted zone in the middle of the goaf is significantly lower than that of the

fracture development zone on both sides. The fracture development zone is the main channel of air seepage in the goaf.

Fig. 12 presents that the permeability coefficient at $Y = 40$ m has an obvious strong correlation with the pore-throat structure parameters, and the goodness of fit is above 0.99 in all cases. The permeability coefficient increases as pore diameter, throat diameter, pore volume and throat volume increase, and increases as throat length decreases. Fig. 12(e) reveals that the correlation between the fitted curves of the permeability coefficient and the throat volume is the highest. Therefore, it can be shown that the throat channel is the main control factor governing the fluid transport capacity. The better the development of the throat channel structure, the stronger the air transport capacity in the goaf.

5. Conclusions

This paper presents a new method to study the flow field and permeability characteristics in the goaf. The PNM method with the OpenPNM package was used to construct a pore network model consisting of pore-throat systems. The network was analyzed using the Stokes flow algorithm combined with the Hagen-Poiseuille law, and the following conclusions were drawn.

(1) Behind the advancing 2220 face in the Linnancang mine, a pore network model in the goaf with pore diameters and throat diameters in the range of 0.025-0.049 m was established by combining the bulking factor distribution of "O-ring" and Weibull distribution. The shape and scale parameters characterizing goaf porosity are 1.41 and 1.244, respectively.

(2) The simulation provided distribution characteristics of air pressure at the pore scale in the goaf of Linnancang mine. The air pressure gradient is the largest near the upper and lower corners of the working face, while the air pressure difference is insignificant in the middle of the working face. The air pressure tends to level off gradually after 120 m along the direction of the goaf, and there is almost no change in pressure at the deeper part of the goaf.

(3) The obtained characteristics of air velocity distribution in the goaf show that air leakage flow lines in the goaf are symmetrical and circular. The flow line density of airflow near the face is greater than in the internal area, especially in the upper and lower corners of the goaf. The air leakage movement pattern is consistent with the changes in the non-compaction zone. The maximum air velocity is 0.011147 m/s.

(4) The transport property of the goaf is directly related to the pore structure of the pore network. The permeability coefficient ranges from 5.32×10^{-4} to 7.78×10^{-3} m^3/(Pa·s) in the goaf of Linnancang mine. The permeability coefficient increases as pore diameter, throat diameter, pore volume and throat volume increase and increases as throat length decreases. The correlation between throat volume and permeability coefficient is the highest, which indicates that the whole throat is the main control factor governing the air transport capacity in the goaf.

Conflict of Interest

The authors declare no competing interests.

References

[1] K. Gao, L.J. Deng, J. Liu, L.X. Wen, D. Wong, Z.Y. Liu, Study on Mine Ventilation Resistance Coefficient Inversion Based on Genetic Algorithm. Arch. Min. Sci. **63** (4), 813-826 (2018).
DOI: https://doi.org/10.24425/ams.2018.124977

[2] J. Szlązak, The Determination of a Co-efficient of Longwall Goaf Permeability. Arch. Min. Sci. **46** (4), 451-468 (2001).

[3] M.G. Qian, J.L. Xu, Study on the "O-shape" Circle Distribution Characteristics of Mining-induced Fractures in the Overlaying Strata. J. China Coal Soc. **23** (5), 466-469 (1998).

[4] S.G. Li, M.G. Qian, P.W. Shi, Study on Bed-separated Fissures of Overlying Stratum and Interstice Permeability in Fully-mechanized Top Coal Caving. Chin. J. Rock Mech. Eng. **19** (5), 604-607 (2000).

[5] Y.T. Liang, T.F. Zhang, S.G. Wang, J.P. Sun, Heterogeneous Model of Porosity in Gobs and Its Airflow Field Distribution. J. China Coal Soc. **34** (9), 1203-1207 (2009).

[6] P. Chen, L. Zhang, G.Q. Zou, Study of Three-dimensional Distribution of Permeability in Goaf Based on O-shape Circle Theory. Min. Saf. Environ. Prot. **42** (5), 38-41 (2015).

[7] G.C. Gao, Z.X. Li, C. Zhang, Y. Zhang, J. Liu, B.D. Wu, Numerical Simulation for Multi-field Distribution Characteristic Features of the Goaf Based on 3D "O" Type Circle. J. Saf. Environ. **17** (3), 931-936 (2017).
DOI: https://doi.org/10.13637/j.issn.1009-6094.2017.03.023

[8] J.H. Si, G.Y. Cheng, J.F. Zhu, T.X. Chu, Three-dimensional Modeling and Application of Permeability Characteristics of Heterogeneous Porous Media in Goaf. Coal Sci. Technol. **47** (5), 220-224 (2019).
DOI: https://doi.org/10.13199/j.cnki.cst.2019.05.035

[9] M.M. Rashidi, A. Hosseini, I. Pop, S. Kumar, N. Freidoonimehr, Comparative Numerical Study of Single and Two-phase Models of Nanofluid Heat Transfer in Wavy Channel. Appl. Math. Mech. **35**, 831-848 (2014).
DOI: https://doi.org/10.1007/s10483-014-1839-9

[10] A. Sohail, H.A. Wajid, M.M. Rashidi, Numerical Modeling of Capillary–gravity Waves Using the Phase Field Method. Surface Review and Letters. **21** (03), 1450036 (2014). DOI: https://doi.org/10.1142/s0218625x1450036x

[11] R. Sadeghi, M.S. Shadloo, M. Hopp-Hirschler, A. Hadjadj, U. Nieken, Three-dimensional Lattice Boltzmann Simulations of High Density Ratio Two-phase Flows in Porous Media. Comput. Math. Appl. **75** (7), 2445-2465 (2018). DOI: https://doi.org/10.1016/j.camwa.2017.12.028

[12] J. Gostick, M. Aghighi, J. Hinebaugh, T. Tranter, M.A. Hoeh, H. Day, B. Spellacy, M.H. Sharqawy, A. Bazylak, A. Burns et al., OpenPNM: A Pore Network Modeling Package. Comput. Sci. Eng. **18** (4), 60-74 (2016).
DOI: https://doi.org/10.1109/mcse.2016.49

[13] K. Xu, W. Wei, Y. Chen, H. Tian, S. Xu, J. Cai, A Pore Network Approach to Study Throat Size Effect on the Permeability of Reconstructed Porous Media. Water **14** (1), (2022). DOI: https://doi.org/10.3390/w14010077

[14] W. Wei, J. Cai, J. Xiao, Q. Meng, B. Xiao, Q. Han, Kozeny-Carman Constant of Porous Media: Insights from Fractal-capillary Imbibition Theory. Fuel **234**, 1373-1379 (2018). DOI: https://doi.org/10.1016/j.fuel.2018.08.012

[15] M.S. Shadloo, G. Oger, D. Le Touzé, Smoothed Particle Hydrodynamics Method for Fluid Flows, towards Industrial Applications: Motivations, Current State, and Challenges. Comput. Fluids **136**, 11-34 (2016).
DOI: https://doi.org/10.1016/j.compfluid.2016.05.029

[16] Z.X. Chen, G.R. Huan, Y.L. Ma, Computational Methods for Multiphase Flows in Porous Media. (2006).

[17] J. Miao, MSc thesis, 3D Reconstruction and Seepage Simulation of Macropores Structure in Low Permeability Coal. Henan University of Technology, Jiaozuo, China (2017).

[18] I. Fatt, The Network Model of Porous Media. Transactions of the AIME. **207** (01), 144-181 (1956).
DOI: https://doi.org/10.2118/574-G

[19] R.G. Larson, L.E. Scriven, H.T. Davis, Percolation Theory of Two Phase Flow in Porous Media. Chem. Eng. Sci. **36** (1), 57-73 (1981). DOI: https://doi.org/10.1016/0009-2509(81)80048-6

[29] M. Agnaou, M.A. Sadeghi, T.G. Tranter, J.T. Gostick, Modeling Transport of Charged Species in Pore Networks: Solution of the Nernst-Planck Equations Coupled With Fluid Flow and Charge Conservation Equations. Comput. Geosci. **140**, 104505 (2020). DOI: https://doi.org/10.1016/j.cageo.2020.104505

[21] J. Bear, Translated by J.S. Li, C.X. Chen, Dynamics of Fluids in Porous Media, China Construction Industry Press, Beijing (1983).

[22] K.E. Thompson, Pore-scale Modeling of Fluid Transport in Disordered Fibrous Materials. AIChE. J. **48** (7), 1369-1389 (2002). DOI: https://doi.org/10.1002/aic.690480703

[23] T.G. Tranter, J.T. Gostick, A.D. Burns, W.F. Gale, Pore Network Modeling of Compressed Fuel Cell Components with OpenPNM. Fuel Cells **16** (4), 504-515 (2016). DOI: https://doi.org/10.1002/fuce.201500168

[24] B.Q. Zhang, Y.X. Wang, Oil (gas) Layer Physics, China University of Geosciences Press, Wuhan (1989).

[25] F. Huang, PhD thesis, Three-dimensional Reconstruction and Simulation of Porous Media, University of Science and Technology of China, Hefei, China (2007).

[26] Z.X. Li, G. Yi, J.G. Wu, D. Guo, C.J. Chun, D. Zhao, Study on spontaneous Combustion Distribution of Goaf Based on the "O" Type Risked Falling and Non-uniform Oxygen. J. China Coal Soc. **37** (3), 484-489 (2012). DOI: https://doi.org/10.13225/j.cnki.jccs.2012.03.031

[27] J.M. Li, MSc thesis, Design and Research of Fire Prevention and Extinguishing Scheme for Nitrogen Injection in Goaf of Fully Mechanized Caving Face in Linnancang Coal Mine, Liaoning Technical University, Fuxin, China (2019).

[28] S.P. Sutera, R. Skalak, The History of Poiseuille's Law. Annu. Rev. Fluid. Mech. **25** (1), 1-20 (1993). DOI: https://doi.org/10.1146/annurev.fl.25.010193.000245

[29] J.T. Gostick, M.A. Ioannidis, M.W. Fowler, M.D. Pritzker, Pore Network Modeling of Fibrous Gas Diffusion Layers For Polymer Electrolyte Membrane Fuel Cells. J. Power Sources **173** (1), 277-290 (2007). DOI: https://doi.org/10.1016/j.jpowsour.2007.04.059

[30] M.A. Ioannidis, I. Chatzis, Network Modeling of Pore Structure and Transport-properties of Porous-media. Chem. Eng. Sci. **48** (5), 951-972 (1993). DOI: https://doi.org/10.1016/0009-2509(93)80333-l

[31] H.L. Gu, X.P. Lai, M. Tao, W.Z. Cao, Z.K. Yang, The Role of Porosity in the Dynamic Disturbance Resistance of Water-saturated Coal. Int. J. Rock Mech. Min. Sci. **166**, 105388 (2023). DOI: https://doi.org/10.1016/j.ijrmms.2023.105388

[32] Z.X. Li, PhD thesis, Study of Limit Coupling Point for Commonlu Controlling Gas and Spontaneous Combustion in Highly Gassy and Spontaneous Combustion Gobs, Liaoning Technical University, Fuxin, China (2007).

[33] J. Szlazak, N. Szlazak, D. Obracaj, M. Borowski, Numerical Determination of Velocity Field of Airflow in Goaf, Proceedings of 31st Biennial International Conference of Safety in Mines Research Institutes: Health and Safety Mining Research for a Sustainable Future, Brisbane, Queensland Australia, 2-5 October 2005, 243-248.